A Novel Optimum Decoupling & Control of MIMO Systems based on Linear Matrix Inequality & Kharitonov Theorem

Sumit Kumar Pandey

***Abstract* — This work presents a discussion of optimal decoupling and control approach for multiple-input multiple-output (MIMO) systems utilizing the contemporary linear matrix inequality (LMI) algorithm. Initially, an approach using optimal decoupling is employed to address the issue of coupling effects in MIMO plants. These effects have the potential to negatively impact the performance of compensated systems. The utilization of the Relative Gain Array (RGA) method is employed in the analysis of MIMO systems to determine the optimal pairing. The LMI approach is commonly utilized to successfully mitigate the coupling effects between input & output of MIMO systems. Furthermore, this paper presents an enhanced proportional integral derivative (PID) control strategy for the resulting system, utilizing the Kharitonov theorem and Bacterial Foraging Optimization (BFO) algorithm. The proposed methodology has been effectively implemented in several MIMO systems, including square, time-delayed, and non-square non-minimum phase configurations. The disturbance rejection performance of the designed controller is also tested through output disturbance rejection. The performance of suggested controller is assessed through simulation results in order to substantiate the theoretical assertions.**

***Index Terms*— MIMO, LMI, Convex optimization, RGA.**

I. Introduction

DURING the period of contemporary industrialization, numerous industrial systems consist of a combination of multiple interacting subsystems. The complexity of the system being considered poses challenges in implementing efficient control mechanisms for various components. The phenomenon wherein an input has an undesirable impact on an output is sometimes referred to as undesired interaction effect. The undesired interaction effects have a detrimental impact on the performance of ensued system. The design of a decoupler is necessary to address the issue of eliminating the coupling effect. The authors in [1] provide a detailed explanation of the decoupling method utilizing optimization techniques to get the required optimal performance of compensated system. The paper demonstrates a methodology that combines decoupling using RGA analysis with Particle Swarm Optimization (PSO) [2]. The right pairing information of MIMO systems which ensures efficient decoupling is elucidated in [3] where RGA is identified as a potent instrument for this purpose. The methodology of utilizing an algebraic approach for decoupling methods is elucidated in reference [4] which discusses the implementation of the output feedback control method. The decoupling technique utilizing the smith predictor methodology is described in [5]. However, it is important to note that this method is constrained to stable MIMO systems, which represents a limitation. In the study in [6] a technique for open loop decoupling is introduced which involves the utilization of a pre-compensator. The application of a static variable state feedback technique has been utilized for achieving total and partial decoupling of MIMO systems [7, 8]. The majority of decoupling approaches documented in academic literature are characterized by their complexity and limited applicability to various types of MIMO plants. The development of a novel decoupling method for a diverse variety of MIMO systems is motivated by a significant factor. Hence, the authors of this study endeavored to devise a decoupling technique for MIMO systems. This method draws upon the disturbance rejection strategy commonly employed in open loop systems. In this study a convex optimization using LMI is employed to minimize the adverse coupling effects that are regarded as disruptions to the intended outputs. The LMI algorithm has found extensive application in control issues, particularly with the advancement of interior point algorithms of the new generation. These algorithms have the capability to efficiently handle problems expressed in the LMI form [9-11]. Another aim is to design PID controller for the decoupled plants obtained. It might be argued that PID controllers continue to be widely utilized in industries due to its inherent simplicity and ease of implementation. The accuracy of a PID controller is contingent upon the appropriate selection of its gain values. Nevertheless, the task of determining controller gain values becomes more challenging when the system characteristics exhibit variability. The utilization of the Kharitonov theorem is employed to construct an appropriate Proportional-Integral-Derivative (PID) controller in situations when the specific physical parameters of the control system are unknown. This theorem is commonly utilized in control system engineering to evaluate the stability of dynamical systems. The aforementioned study establishes the essential and comprehensive criteria for ascertaining the robust stability of polynomials that have been subject to perturbations in their coefficients [12]. The utilization of the Kharitonov theory has proven to be effective in determining the resilient interval of gains for PID controller settings [13-14]. The Kharitonov theorem guarantees that the system under investigation will remain robustly stable within the

Manuscript received July 17, 2024; revised March 5, 2025.

Sumit Kumar Pandey is an Assistant Professor in Department of Electrical and Electronics Engineering, at Amrita School of Engineering, Coimbatore, Amrita Vishwa Vidyapeetham, India (e-mail: p_sumitkumar@cb.amrita.edu).

range of controller gains specified, as indicated by previous research [15-16]. An important goal is to ensure that gain values are appropriately optimized, necessitating the efficient tuning of PID controllers. The authors offer an optimization approach for tuning PID controllers.

Rest of this work is organized as below in which following part deals with the decoupling followed by development of a control algorithm and its application in different types of MIMO systems. Conclusion is narrated in the last section.

II. PROPOSED DECOUPLING METHOD

Let us consider nxn MIMO plant $G(s)$ as shown in Fig. 1 described by equation (1) in which the outputs are y_1, y_2 ...., y_n and inputs are u_1, u_2 ...., u_n. n as written by equation (2).

$$G(s) = \begin{bmatrix} G_{11}(s) & G_{12}(s) & \cdots & G_{1n}(s) \\ G_{21}(s) & G_{22}(s) & \cdots & G_{2n}(s) \\ \cdots & \cdots & \cdots & \cdots \\ G_{n1}(s) & G_{n2}(s) & \cdots & G_{nn}(s) \end{bmatrix} \quad (1)$$

$$\begin{bmatrix} y_1 \\ y_2 \\ \vdots \\ y_n \end{bmatrix} = \begin{bmatrix} G_{11}(s) & G_{12}(s) & \cdots & G_{1n}(s) \\ G_{21}(s) & G_{22}(s) & \cdots & G_{2n}(s) \\ \cdots & \cdots & \cdots & \cdots \\ G_{n1}(s) & G_{n2}(s) & \cdots & G_{nn}(s) \end{bmatrix} \cdot \begin{bmatrix} u_1 \\ u_2 \\ \vdots \\ u_n \end{bmatrix} \quad (2)$$

$$\left.\begin{aligned} y_1 &= G_{11}(s).u_1 + G_{12}(s)u_2 + \ldots + G_{1n}(s)u_n \\ y_2 &= G_{21}(s)u_1 + G_{22}(s)u_2 + \ldots + G_{2n}(s)u_n \\ &\vdots \\ y_n &= G_{n1}(s)u_1 + G_{n2}(s)u_2 + \ldots + G_{nn}(s)u_n \end{aligned}\right\} \quad (3)$$

The equations for individual outputs are defined by equation (3), which illustrates that each output is associated with distinct inputs. Furthermore, each output is dependent on all inputs that have been induced. To effectively develop a control method for MIMO system, it is advantageous to establish a relationship where a specific output is solely influenced by a single input. This can be achieved by employing pairing analysis, which utilizes the Relative Gain Array (RGA) technique. The RGA technique holds significant value as an analytical tool for identifying the optimal pairing between inputs and outputs in MIMO systems. For instance, let us consider the output that is associated with the input in accordance with RGA analysis. In this study, it is assumed that all inputs, except for the specified input, are regarded as disturbances to the output.

Fig. 1. MIMO Plant

A. *Pairing analysis employing RGA*

RGA is a gain matrix which is determined to measure undesired coupling of MIMO systems. If system of transfer function $G(s)$ is considered with n inputs and n outputs, then there exists $n \times n$ having λ_{ij}, which in turn RGA matrix below.

$$\Lambda = \begin{bmatrix} \lambda_{11} & \lambda_{12} & \cdots & \lambda_{1n} \\ \lambda_{21} & \lambda_{22} & \cdots & \lambda_{2n} \\ \cdots & \cdots & & \cdots \\ \lambda_{n1} & \lambda_{n2} & \cdots & \lambda_{nn} \end{bmatrix} \quad (4)$$

$\lambda_{ij}$is defined as below,

$$\lambda_{ij} = \frac{g_{ij}^o}{g_{ij}^c} \quad (5)$$

Whereg_{ij}^o and g_{ij}^c are gains of the transfer function $G_{ij}(s)$ in open & closed loop. As a first case, it is considered that except u_j , all other inputs $u_{k(k=1,2,\ldots,p,k\neq j)}$ are absent, and a step change of magnitude Δu_j in input u_j will produce a change Δy_i of the output y_i. Hence, when all other inputs are absent, the gain between input u_j and output y_i is calculated as g_{ij}^0 which is given by.

$$g_{ij}^o = \left.\frac{\Delta y_i}{\Delta u_j}\right|_{u_k=0} (j \neq k) \quad (6)$$

In the second case, if it is considered that except y_i , all other outputs y_l, $(l = 1,2, \ldots p, l \neq i)$, are zeros, then a step change of magnitude Δu_jin input u_j will result in another change of y_i. However, under this condition, the output y_i is also affected by the other inputs due to cross-coupling. The ratio between input and output can be written as below.

$$g_{ij}^c = \left.\frac{\Delta y_i}{\Delta u_j}\right|_{y_l=0} (i \neq l) \quad (7)$$

Despite the fact that the gains shown above are between the same two factors, but it leads to different values since it is evaluated under different conditions. It can be stated that undesired pairing occurred, the change in $y_i$due to a change in $u_j$for the two cases (when other inputs and when other outputs are kept zeros) are different.

$$\lambda_{ij} = \frac{\left.\frac{\Delta y_i}{\Delta u_j}\right|_{u_k=0} (j \neq k)}{\left.\frac{\Delta y_i}{\Delta u_j}\right|_{y_l=0} (i \neq l)} \quad (8)$$

The above ratio defines the relative gain between the output $y_i$and inputu_j.

Here if $\lambda_{ij} = 0$, the j^{th} input has no effect on y_i output and if $\lambda_{ij} = 1$ in $y_i$only $u_j$effects. Generally, the RGA of the system $G(s)$ can be determined as frequency dependent function, which is given by

$$\Lambda(s) = G(s) .* (G(s)^{-1})^T \quad (9)$$

The effect of other inputs on a particular output except from the corresponding input is termed as disturbance or coupling effect. The main objective of designing a decoupler is to eliminate undesired interactions. In pairing analysis, RGA of

MIMO system matrix is calculated and the corresponding maximum gain of each row of the matrix is fixed to one in the decoupling matrix to signify that the particular output is completely dependent on an individual input only.

B. Decoupling Matrix

The structure of the decoupler is as described in (10), if through the pairing analysis it is found that corresponding gain of $G_{11}$is more than that ofG_{12},G_{13}….. G_{1n} , then $d_{11}$is fixed to 1 such that first output is solely dependent on the first input. If the corresponding gain of G_{22} is more thenG_{21}, G_{23},……,G_{2n}then the decoupling matrix element is d_{22} fixed to 1 in a way that 2nd output is completely dependent on 2nd input. Similarly, if the corresponding gain of G_{nn} is more thenG_{n1}, G_{n2},……,$G_{n.(n-1)}$ then the decoupling matrix element is d_{nn} fixed to 1 in a way that nth output is completely dependent on nth input. With the aforesaid logic the structure of a decoupler is written as equation (11) such thatY_1,Y_2….. $Y_n$is completely influenced by U_1,U_2…. U_n, respectively.

$$D = \begin{bmatrix} d_{11} & d_{12} & \dots & d_{1n} \\ d_{21} & d_{22} & \dots. & d_{2n} \\ \vdots & \vdots & \dots. & \vdots \\ d_{n1} & d_{n2} & \dots. & d_{nn} \end{bmatrix} \quad (10)$$

$$D = \begin{bmatrix} 1 & d_{12} & \dots & d_{1n} \\ d_{21} & 1 & \dots. & d_{2n} \\ \vdots & \vdots & \dots. & \vdots \\ d_{n1} & d_{n2} & \dots. & 1 \end{bmatrix} \quad (11)$$

The new decoupled plant$G_N(s)$ is written as

$$G_N(s) = \begin{bmatrix} G_{11}(s) & G_{12}(s) & \dots. & G_{1n}(s) \\ G_{21}(s) & G_{22}(s) & \dots. & G_{2n}(s) \\ \vdots & \vdots & \vdots & \vdots \\ G_{n1}(s) & G_{n2}(s) & \dots.. & G_{nn}(s) \end{bmatrix} . \begin{bmatrix} 1 & d_{12} & \dots & d_{1n} \\ d_{21} & 1 & \dots. & d_{2n} \\ \vdots & \vdots & \vdots & \vdots \\ d_{n1} & d_{n2} & \dots. & 1 \end{bmatrix} \quad (12)$$

$$\begin{bmatrix} G_{11}(s)+.+G_{1n}(s)d_{n1} & G_{11}(s)d_{12}+.+G_{1n}(s)d_{n2} & .. & G_{11}(s)d_{1n}+.+G_{1n}(s) \\ G_{21}(s)+.+G_{2n}(s)d_{n1} & G_{21}(s)d_{12}+.+G_{2n}(s)d_{n2} & .. & G_{n1}(s)d_{1n}+.+G_{2n}(s) \\ \vdots & \vdots & \vdots & \vdots \\ G_{n1}(s)+.+G_{nn}(s)d_{n1} & G_{n1}(s)d_{12}+.+G_{nn}(s)d_{n2} & .. & G_{n1}(s)d_{1n}+.+G_{nn}(s) \end{bmatrix} \quad (13)$$

The corresponding outputs are written as equation (14) where it is seen clearly that for any MIMO system one output is influenced by all the inputs.

$$\begin{gathered} Y_1 = (G_{11}(s) + G_{12}(s)d_{21} + \cdots. + G_{1n}(s)d_{n1}).V_1 \\ +(G_{11}(s)d_{12} + G_{12}(s) + \cdots. + G_{1n}(s)d_{n2}).V_2 + \cdots. \\ +(G_{11}(s)d_{1n} + G_{12}(s)d_{2n} + \dots. + G_{1n}(s)).V_n \\ \\ Y_2 = (G_{21}(s) + G_{22}(s)d_{21} + \cdots. + G_{2n}(s)d_{n1}).V_1 \\ +(G_{21}(s)d_{12} + G_{22}(s) + \cdots. + G_{2n}(s)d_{n2}).V_2 + \cdots. \\ +\left(G_{n1}(s)d_{1n} + G_{n2}(s)d_{2n} + \cdots. + G_{2n}(s)\right).V_n \\ \vdots \\ Y_n = (G_{n1}(s) + G_{n2}(s)d_{21} + \cdots. + G_{nn}(s)d_{n1}).V_1 \\ +(G_{n1}(s)d_{12} + G_{n2}(s) + \cdots. + G_{nn}(s)d_{n2}).V_2 + \cdots. \\ +(G_{n1}(s)d_{1n} + G_{n2}(s)d_{2n} + \dots. + G_{nn}(s)).V_n \end{gathered} \quad (14)$$

The decoupling technique is interpreted as a convex constrained optimization problem in which the decoupling gain is obtained to minimize the objective function as described by equation (14) where it is desired that a particular output should influenced by the corresponding input only whose RGA is highest among all. The influence of other inputs on that particular output is treated as a disturbance and effect of this disturbance is minimized by using LMI approach.

C. Linear Matrix Inequality

A LMI is defined as,

$$F(X) = F_0 + F_1x_1 + F_2x_2 + \dots. + F_nx_n < 0 \quad (15)$$

Where, $X = (x_1, x_2, \dots. x_n)$ is a vector of unknown decisional or optimization variables and $F_0, F_1, F_2, \dots.., F_n$ are assigned symmetrical matrices. Finding the solution of equation (15) is known as a convex optimization problem [17-22]. An optimization problem consists of finding a minimum or maximum value in certain regions defined by certain constraints on the independent variables. If the conditions of a convex optimization problem is written as,

$$\left.\begin{aligned} &F_1(X) < 0 \\ &F_2(X) < 0 \\ &\vdots \\ &F_n(X) < 0 \end{aligned}\right\} \quad (16)$$

Then equation (16) is represented by one single LMI as below,

$$F(X) = \begin{bmatrix} F_1(X) & 0 & \cdots & 0 \\ 0 & F_2(X) & \cdots & 0 \\ \vdots & \vdots & \ddots & \vdots \\ 0 & 0 & \dots & F_n(X) \end{bmatrix} < 0 \quad (17)$$

For convenience the detail procedure for minimizing the coupling effect by implementing LMI algorithm is described as below.

Step 1: Initialization of LMI function and its description.
The LMI function is initialized and the formulation of the LMI problem does not depend on the type of problem rather it is completely generalized. Plant can be represented through A, B, C & D matrix and should be obtained before the initialization of LMI function.

Step 2: Defining the decision variable of LMI in the form of structure & matrix.
It is necessary to define the decisional variables at the time of the initialization of the LMI problem. The decisional matrix consists of type and structure. The matrix may be symmetrical matrices, rectangular matrices etc. For type one the matrix should be square and symmetrical, for type two it should be rectangular.

Step 3: Defining the different LMI conditions and arguments one by one.
The LMI inequality is characterized by defining each of its constituent terms. The value of γ is suitably chosen to achieve the desired performance.

Step 4: Checking the feasibility of the solution.
For solving LMI problem first stability and feasibility of the problem is determined by calculating the feasible solution. The state $x = 0$ of the system $\dot{x} = A(x)$ is asymptotically stable if there is a matrix $P > 0$ which satisfies$A^TP + PA < 0$. The LMI problem is feasible if the system is asymptotically

stable. The condition is represented as below to be satisfy to ensure the stability and feasibility of a LTI system.

$$P > 0$$

$$\begin{bmatrix} A^T P + PA & PB - C^T \\ B^T P - C & -D^T - D \end{bmatrix} \leq 0 \quad (18)$$

Step 5: Determining the solution of the problem using LMI solver.
The generalized form of the linear convex optimization problem is considered as to find the minimum value of λ that minimizes the objective function while satisfying the constraints [16]. The constraints are classified as the linear inequality constraints.

$$\left.\begin{aligned} A(x) < \lambda B(x) \\ B(x) > 0 \\ C(x) < 0 \end{aligned}\right\} \quad (19)$$

The interior point optimization algorithms developed by Nesterov and Nemirovski [11] provide an efficient method to solve the generically LMI problems. The inequality is formulated as linear matrix inequality which is termed as generalized eigenvalue minimization problem.

$$P > 0$$

$$\begin{bmatrix} A^T P + PA + C^T C & PB \\ B^T P & 0 \end{bmatrix} \leq \alpha^2 \begin{bmatrix} \gamma I & 0 \\ 0 & I \end{bmatrix} \quad (20)$$

γ is the quantity introduced to get the numerical solution of the problem, if the value of γ is near to zero, it causes a slow convergence and if its value is high the desired performance is not guaranteed. Therefore γ is chosen suitably to tradeoff between guaranteed performance and slow convergence. α is the H_∞ norm of the system $G(s) = C(sI - A)^{-1}B$.

D. Steps for the design of decoupler

Following are the different steps adopted for the design of decoupler.
Step 1: Best paired interconnection is selected on the basis of RGA technique for the given MIMO plant.
Step 2: Transfer matrix of the MIMO system is converted into the state space form so that LMI can be easily implemented.
Step 3: Apart from the best-paired interaction the gain of other interactions are minimized using LMI technique described above.
Step 4: After following the above steps the achieved decoupler gain values are represented as Equation (11).

E. Example

The following section implements the suggested decoupling techniques while taking various MIMO plant types into consideration. To get the desired response after the decoupling closed loop control is required. In this direction PID controller is designed using Kharitonov theorem [13,14] in next section.

Square Time delayed MIMO System

A square time delayed MIMO system having the transfer function as below is considered first to implement the proposed method.

$$G(s) = \begin{bmatrix} G_{11}(s) & G_{12}(s) \\ G_{21}(s) & G_{22}(s) \end{bmatrix} = \begin{bmatrix} \frac{12.8e^{-s}}{16.7s+1} & \frac{-18.9e^{-3s}}{21s+1} \\ \frac{6.6e^{-7s}}{10.9s+1} & \frac{-19.4e^{-3s}}{14.4s+1} \end{bmatrix} (21)$$

The relative gain array of the MIMO system is calculated as below

$$RGA = \begin{bmatrix} 2.0094 & -1.0094 \\ -1.0094 & 2.0094 \end{bmatrix} \quad (22)$$

It is signifying by the relative gain analysis that 1st output should paired with 1st input & 2nd output is paired with 2nd input. Hence the structure of decoupler is written as below

$$D = \begin{bmatrix} 1 & d_{12} \\ d_{21} & 1 \end{bmatrix} \quad (23)$$

By using the equation below, the decoupled system with the decoupler matrix is expressed as follows (12).

$$\mathrm{G_N(s)} = \begin{bmatrix} \frac{12.8e^{-s}}{16.7s+1} & \frac{-18.9e^{-3s}}{21s+1} \\ \frac{6.6e^{-7s}}{10.9s+1} & \frac{-19.4e^{-3s}}{14.4s+1} \end{bmatrix} \begin{bmatrix} 1 & d_{12} \\ d_{21} & 1 \end{bmatrix} (24)$$

$$\begin{bmatrix} \frac{12.8e^{-s}}{16.7s+1} + \frac{-18.9e^{-3s}}{21s+1} d_{21} & \frac{12.8e^{-s}}{16.7s+1} d_{12} + \frac{-18.9e^{-3s}}{21s+1} \\ \frac{6.6e^{-7s}}{10.9s+1} + \frac{-19.4e^{-3s}}{14.4s+1} d_{21} & \frac{6.6e^{-7s}}{10.9s+1} d_{12} + \frac{-19.4e^{-3s}}{14.4s+1} \end{bmatrix}$$

(25)

$$Y_1 = \left(\frac{12.8e^{-s}}{16.7s+1} + \frac{-18.9e^{-3s}}{21s+1} d_{21} \right). V_1 + \left(\frac{12.8e^{-s}}{16.7s+1} d_{12} + \frac{-18.9e^{-3s}}{21s+1} \right). V_2 (26)$$

$$Y_2 = \left(\frac{6.6e^{-7s}}{10.9s+1} + \frac{-19.4e^{-3s}}{14.4s+1} d_{21} \right). V_1 + \left(\frac{6.6e^{-7s}}{10.9s+1} d_{12} + \frac{-19.4e^{-3s}}{14.4s+1} \right). V_2$$

(27)

The corresponding outputs are calculated as below following the equation (14) in which the effect of input V_2 is act as a disturbance for output Y_1 as described in equation (26) and effect of input V_1 is act as a disturbance for output Y_2 as described in equation (27). The goal is to reduce both the disruption and the issue is considered as a generalized eigenvalue minimization problem for the corresponding gain value of d_{12}&d_{21}. In this problem the range of d_{12}&d_{21} are taken in between 0.0001 to 1 and for individual gain the eigenvalue is calculated. It is found that the gain value is minimum for d_{12} is obtained as 0.25 &d_{21} is as 0.0002.

Non-square Non-minimum Phase System

A non-square MIMO system having the transfer function as below is also considered to test the proposed decoupling control method. The plant considered here is of non-minimum phase type which make the system more complex for design the controller. In this also the pairing analysis is calculated to know the best paring between inputs and outputs of the MIMO system using RGA.

$$G(s) = \begin{bmatrix} \frac{4}{20s+1} & \frac{2}{20s+1} & \frac{4s-2}{20s+1} \\ \frac{3s-3}{10s+1} & \frac{3}{10s+1} & \frac{5s-1}{10s+1} \end{bmatrix} \quad (28)$$

The relative gain array of the MIMO system is calculated as below

$$RGA = \begin{bmatrix} 0.5818 & 0.2273 & 0.1909 \\ 0.3818 & 0.5455 & 0.0727 \end{bmatrix} \quad (29)$$

It is signified by the relative gain analysis that 1st output should paired with 1st input and 2nd output with 2nd input. Hence the structure of decoupler is written as below

$$D = \begin{bmatrix} 1 & d_{12} \\ d_{21} & 1 \\ d_{31} & d_{32} \end{bmatrix} \quad (30)$$

Hence the decoupled system is designed as

$$G_N(s) = \begin{bmatrix} \frac{4}{20s+1} & \frac{2}{20s+1} & \frac{4s-2}{20s+1} \\ \frac{3s-3}{10s+1} & \frac{3}{10s+1} & \frac{5s-1}{10s+1} \end{bmatrix} . \begin{bmatrix} 1 & d_{12} \\ d_{21} & 1 \\ d_{31} & d_{32} \end{bmatrix} \quad (31)$$

The corresponding outputs are calculated as below following the equation (14) in which the input $V_2$is act as a disturbance for output Y_1as described in equation (32) and input $V_1$is act as a disturbance for output Y_2as described in equation (33).

$$Y_1 = \left(\frac{4}{20s+1} + \frac{2}{20s+1} d_{21} + \frac{4s-2}{20s+1} d_{31}\right). V_1 + \left(\frac{4}{20s+1} d_{12} + \frac{2}{20s+1} + \frac{4s-2}{20s+1} d_{32}\right). V_2 \quad (32)$$

$$Y_2 = \left(\frac{3s-3}{10s+1} + \frac{3}{10s+1} d_{21} + \frac{5s-1}{10s+1} d_{31}\right) V_1 + \left(\frac{3s-3}{10s+1} d_{12} + \frac{3}{10s+1} + \frac{5s-1}{10s+1} d_{32}\right). V_2 \quad (33)$$

The problem is optimized in the similar fashion as discussed in previous example. In this problem there are four variables to be optimized with the two equations hence in order to achieve the optimum performance first two gain values are fixed one from each equation as d_{31}&$d_{32}$is -1. After those the other two values of the gains are determined by the following the procedure of LMI algorithm and the value of $d_{12}$is obtained as -0.6651 &$d_{21}$is as -0.9804.

III. CONTROLLER DESIGN

Although a conclusion may review the main points of the paper, do not replicate the abstract as the conclusion. A conclusion might elaborate on the importance of the work or suggest applications and extensions. The performance of any system depends only on the designing of effective controllers [26-29,31-34]. PID control scheme using Kharitonov method of n^{th} subsystem of decoupled MIMO plant is shown in Fig. 2. Kharitonov method is applied for understanding robust performance of the designed compensated system. [15] described a stability theorem, known as Kharitonov stability theorem, for classes of polynomial defined by choosing each element independently in a class of specified region. This theorem demonstrates the important finding that four well-defined polynomials must be stable in order for the entire class of polynomials to be Hurwitz stable. Another name for these polynomials is interval polynomials. Only when every member of a set of polynomials is a Hurwitz polynomial can the set be considered stable. Let us examine the collection of $p(s)$ real polynomials of degree in the following form:

$$\delta(s) = \delta_0 + \delta_1 s + \delta_2 s^2 + \delta_3 s^3 + \delta_4 s^4 + \ldots\ldots\ldots \delta_n s^n \quad (34)$$

In this case, the coefficient falls inside a specific range as, $\delta_0 \in [x_0, y_0], \delta_1 \in [x_1, y_1], \ldots\ldots \delta_n \in [x_n, y_n]$. In this instance a polynomial $\underline{\delta} = [\delta_0 + \delta_1, \ldots\ldots., \delta_n]$ and its coefficient vector were discovered as $\Delta = \{\underline{\delta}: \in IR^{n+1}, x_i \leq \delta_i \leq y_i, i = 0,1,2, \ldots\ldots. n\}$. Following Kharitonov theorem in each polynomial the set $p(s)$ is Hurwitz if and only if following extreme polynomial will be stable.

$$K_1(s) = x_0 + x_1 s + y_2 s^2 + y_3 s^3 + x_4 s^4 + x_5 s^5 + y_6 s^6 + \ldots\ldots,$$

$$K_2(s) = x_0 + y_1 s + y_2 s^2 + x_3 s^3 + x_4 s^4 + y_5 s^5 + y_6 s^6 + \ldots\ldots,$$

$$K_3(s) = y_0 + x_1 s + x_2 s^2 + y_3 s^3 + y_4 s^4 + x_5 s^5 + x_6 s^6 + \ldots\ldots,$$

$$K_4(s) = y_0 + y_1 s + x_2 s^2 + x_3 s^3 + y_4 s^4 + y_5 s^5 + x_6 s^6 + \ldots\ldots, \quad (35)$$

The Kharitonov theorem, as mentioned above, is applied for controller design for each of the two transfer functions [13–14]. The characteristic equation for each transfer function is determined along with the transfer function of PID controller. After that following (36) interval equations are written with lower and upper controller values. To get the values of controller parameters one parameter is assumed first and rest two are obtained by satisfying [13, 14] the conditions of interval polynomials described by equation (35). In order to get the optimized performance of the PID controller with guaranteed stability, fine tuning of the controller parameters as accomplished with the help of BFO within the obtained range of Kharitonov theorem [13]. The flow chart of BFO optimization is shown in Figure 3. It is widely acknowledged that performance of BFO is dependent on cost function and also the performance of PID controller depends on the gain values. Therefore, it is important to fix the cost function very wisely. In this work the cost function is taken as below [13,14].

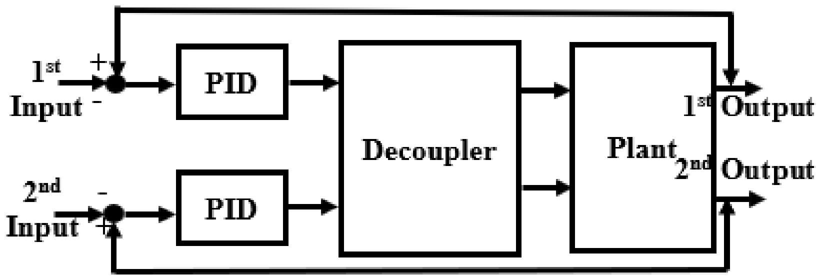

Fig. 2. Decoupled PID control scheme

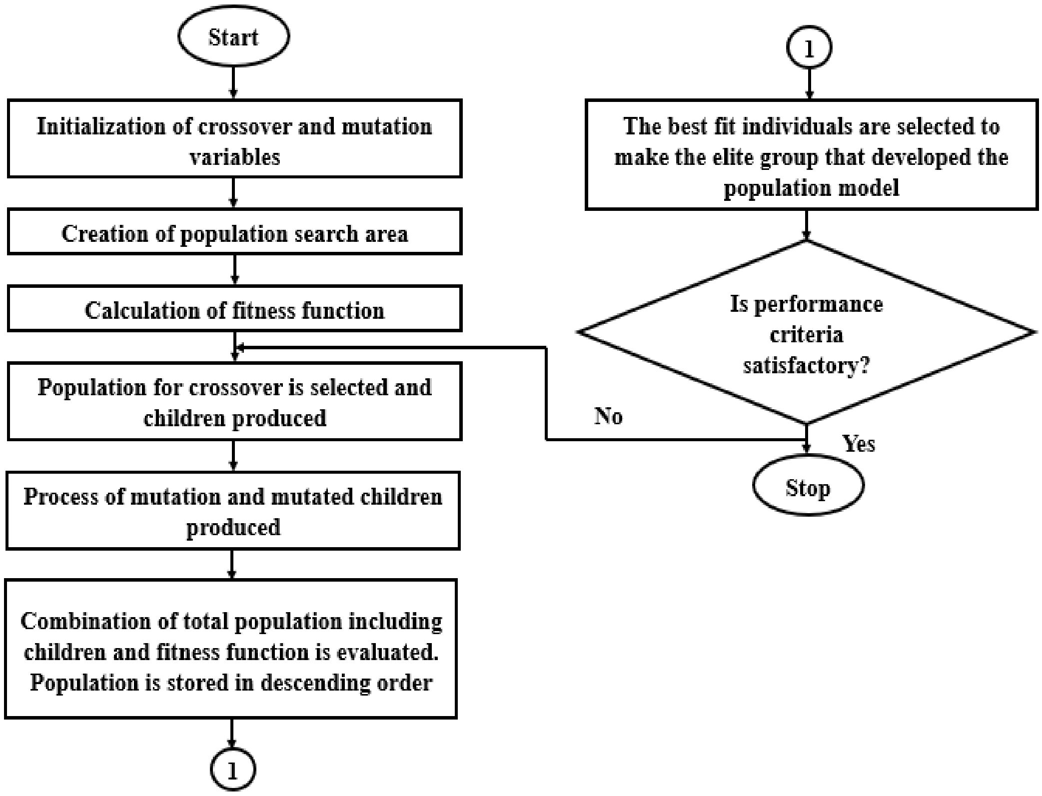

Fig. 3. BFO algorithm flow chart

$$Cost - function = (1 - e^{-\beta})(M_p + E_{ss}) + e^{-\beta}(t_s - t_r) \tag{36}$$

To test the proposed decoupling control method as stated in above sections is implemented through the various examples considered in previous section. In this a square time delayed MIMO system is considered first in section than the non-square non-minimum phase system.

A. Square Time delayed Decoupled System

To implement the Kharitonov theorem, the decoupled transfer function as described in section 2.5.1 of the time delayed system is first rationalized on the basis of first order pade approximation method [29]. In case of $G_{11}(s)$ the rational transfer function can be written as

$$G_{11}(s) = \frac{12.8e^{-s}}{16.7s+1} = \frac{12.8}{16.7s+1} \times \frac{1-0.5s}{1+0.5s} = \frac{-6.4s+12.8}{8.35s^2+17.2s+1} \tag{37}$$

Similarly, for $G_{22}(s)$ the rational transfer function can be written as

$$G_{22}(s) = \frac{-19.4e^{-3s}}{14.4s+1} = \frac{-19.4}{14.4s+1} \times \frac{(e^{-0.75s})^2}{(e^{0.75s})^2}$$

$$= \frac{-19.4}{14.4s+1} \times \frac{(1-0.75s)^2}{(1+0.75s)^2}$$

$$= \frac{-19.4 + 29.1s - 10.91s^2}{1 + 15.9s + 22.16s^2 + 8.06s^3} \tag{38}$$

The PID controller's loop transfer function is expressed for $G_{11}(s)$ is as below,

$$G_{L11}(s) = G_{11}(s).G_{c1}(s)$$

$$= \left[\frac{\begin{array}{c}-6.4K_{d1}s^3 - s^2[6.4K_{p1} - 12.8K_{d1}] \\ +s[12.8K_{p1} - 6.4K_{i1}] + 12.8K_{i1}\end{array}}{8.35s^3 + 17.2s^2 + s}\right] \tag{39}$$

And that for $G_{22}(s)$ is written as

$$G_{L22}(s) = G_{22}(s).G_{c2}(s)$$
$$= \left[\frac{\begin{matrix}-10.91K_{d2}s^4 + s^3[-10.9K_{p2} + 29.1K_{d2}] \\ +s^2[-10.91K_{i2} + 29.1K_{p2} - 19.4K_{d2}] \\ +s[29.1K_{i2} - 19.4K_{p2}] - 19.4K_{i2}\end{matrix}}{8.06s^4 + 22.16s^3 + 15.9s^2 + s}\right] \quad (40)$$

Characteristic equation is written below for $G_{L11}(s)$

$$s^3[8.35 - 6.4K_{d1}]$$
$$+s^2[17.2 - 6.4K_{p1} + 12.8K_{d1}]$$
$$+s[1 - 6.4K_{i1} + 12.8K_{p1}] + 12.8K_{i1} = 0 \quad (41)$$

For finding the robustness of designed controller, an interval is used to represent the system's characteristic polynomial as $[K_{p1}^{-}K_{p1}^{+}]$, $[K_{i1}^{-}K_{i1}^{+}]$, $[K_{d1}^{-}K_{d1}^{+}]$ for K_{p1},K_{i1}&K_{d1} , respectively, in the characteristic polynomial. Then, the four interval polynomials associated with the Kharitonov characteristic is obtained as below. In order to find the values of controller parameter, one parameter is suitably assumed, after which the remaining two parameters are determined by meeting and solving equation (35).

$$K_1(s) = 12.8K_{i1}^{-} + s[1 - 6.4K_{i1}^{-} + 12.8K_{p1}^{-}]$$
$$+s^2[17.2 - 6.4K_{p1}^{+} + 12.8K_{d1}^{+}] + s^3[8.35 - 6.4K_{d1}^{+}]$$

$$K_2(s) = 12.8K_{i1}^{-} + s[1 - 6.4K_{i1}^{+} + 12.8K_{p1}^{+}]$$
$$+s^2[17.2 - 6.4K_{p1}^{+} + 12.8K_{d1}^{+}] + s^3[8.35 - 6.4K_{d1}^{-}]$$

$$K_3(s) = 12.8K_{i1}^{+} + s[1 - 6.4K_{i1}^{-} + 12.8K_{p1}^{-}]$$
$$+s^2[17.2 - 6.4K_{p1}^{-} + 12.8K_{d1}^{-}] + s^3[8.35 - 6.4K_{d1}^{+}]$$

$$K_4(s) = 12.8K_{i1}^{+} + s[1 - 6.4K_{i1}^{+} + 12.8K_{p1}^{+}]$$
$$+s^2[17.2 - 6.4K_{p1}^{-} + 12.8K_{d1}^{-}] + s^3[8.35 - 6.4K_{d1}^{-}] \quad (42)$$

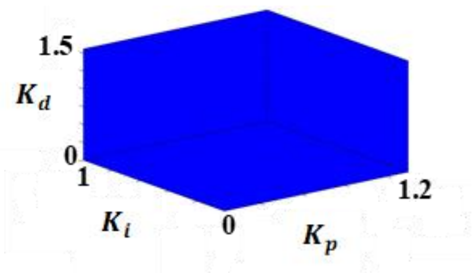

(a) For $G_{L11}(s)$

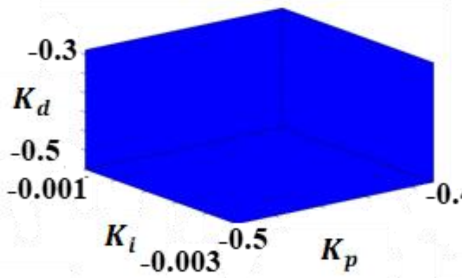

(b) For $G_{L22}(s)$

Fig. 4 PID gain value range of square time delayed decoupled system

The values of the controller gain thus found out are shown in Fig. 4(a). Similar process is adopted to determine the PID gain values for $G_{L22}(s)$ are also shown by Figure 4(b). The simulation is performed with the obtained gain value and found that there is no effect of coupling is present as displayed in Fig. 5. wherein the first input receives a step signal and no input is applied to 2nd input portrayed in Fig. 5 (a) where it is observed from the figure that only first output is obtained and zero output is found on 2nd output. Similarly, in second case step signal is applied in second input and no signal is applied to first input, it is observed that only the output response for second is shown and first remains zero displayed in Fig. 5(b).

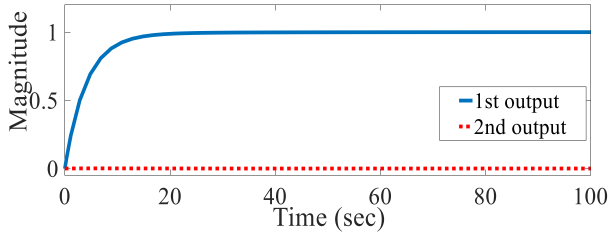

(a) Step reaction of first output and interaction in second because of the first's step input

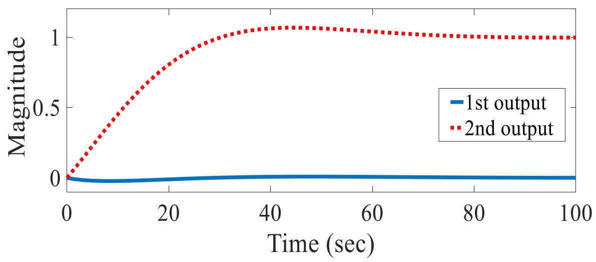

(b) Step reaction of second output and the interaction in first because of the second's step input

Fig. 5 Coupling effect for square time delayed decoupled system

The simulation is performed with the optimized robust PID controller gains which are determined by Kharitonov theorem and optimized by BFO method. The loop transfer function of $G_{11}(s)$ &$G_{22}(s)$ with the optimized values of PID controller parameters are written as $G_{L11}(s)$ &$G_{L22}(s)$, respectively.

$$G_{L11}(s) = \left[\frac{-8s^3+35.66s^2+5.42s+0.09}{8.35s^3+17.2s^2+s}\right] \quad (43)$$

$$G_{L22}(s) = \left[\frac{5.35s^4-12.73s^3+5.46s^2+2.636s+0.05}{8.06s^4+22.16s^3+15.9s^2+s}\right] \quad (44)$$

Fig. 5 verifies that the plant is perfectly decoupled as there is no effect of one input to other output. When both inputs get the step input at the same time, Fig. 6 illustrates the step response and control signal analysis for each output. The output response shown in Fig. 6 (a) is satisfactory with respect to time response as there is no overshoot and settling time is also very less for such types of system. Fig. 6 (b) depicts the time response description of both the outputs. Control signals applied for both the outputs are portrayed in Fig. 6(c). The response of first output with and without the incorporation of decoupler is presented in Fig. 6(d) and the bar charts displayed in Fig. 6 (e) shows the comparative analysis of the output ressponses. Similarly the second output responses with and without decouplers are shown in Fig. 6(f) and the respective bar chart analysis is portrayed in Fig. 6(g). Time response analysis of the first and second outputs for square time delayed decoupled system is tabulated in Table I. In Table II time response analysis of first output with and without decoupler for square time delayed decoupled system is tabulated. Table III depicts the time response analysis of second output with and without decoupler for square time delayed decoupled system.

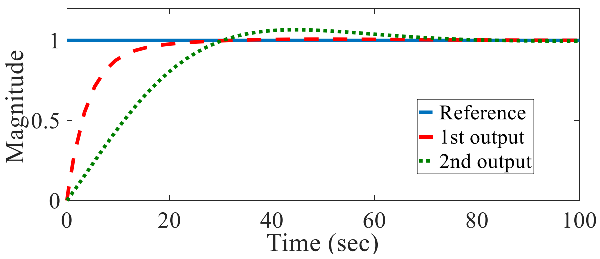

(a) Step response of the first and second outputs

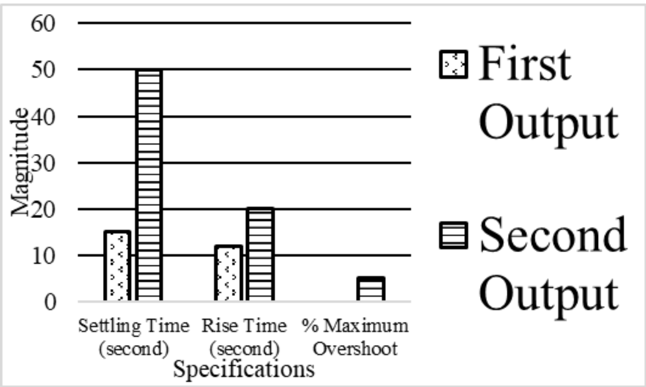

(b) Graphical analysis of the first and second outputs

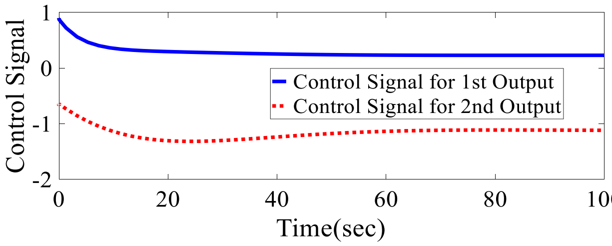

(c) Control Signal for first and second outputs

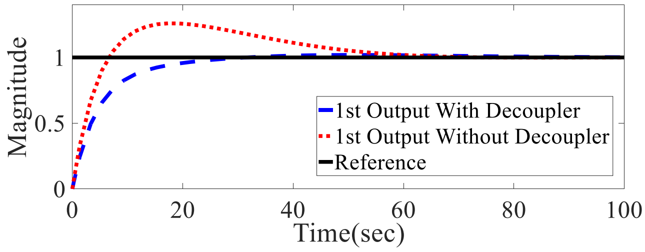

(d) Step response of the first output with and without decoupler

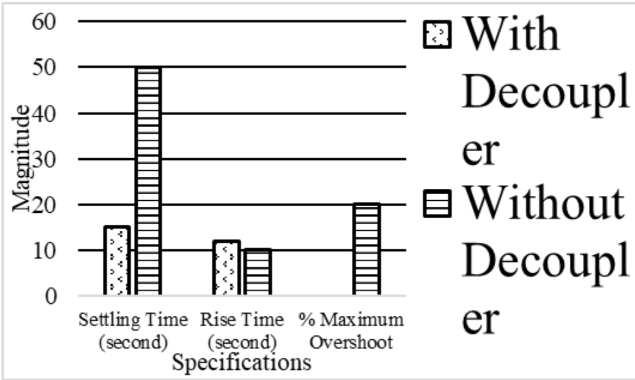

(e) Graphical analysis of first output with and without decoupler

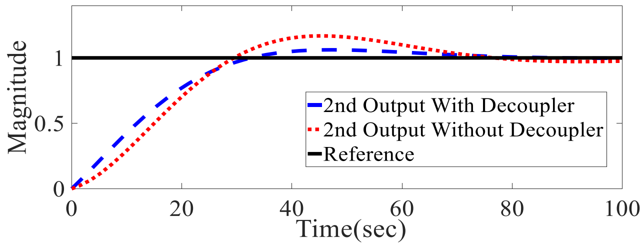

(f) Step response of the second output with and without decoupler

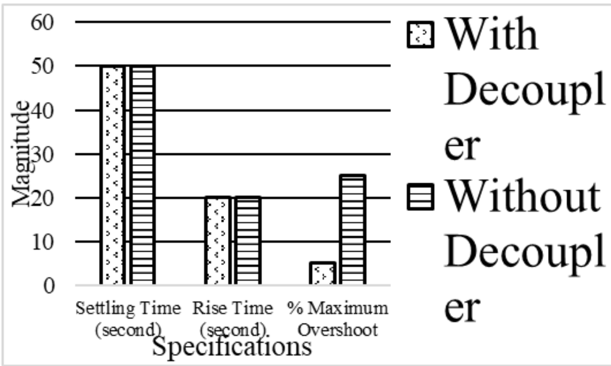

(g) Graphical analysis of second output with and without decoupler

Fig. 6 Time response analysis of square time delayed decoupled system

TABLE I
TIME RESPONSE ANALYSIS OF THE FIRST AND SECOND OUTPUTS FOR SQUARE TIME DELAYED DECOUPLED SYSTEM

Specifications	First Output	Second Output
Settling Time (second)	15	50
Rise Time (second)	12	20
% Maximum Overshoot	0	5

TABLE II
TIME RESPONSE ANALYSIS OF FIRST OUTPUT WITH AND WITHOUT DECOUPLER FOR SQUARE TIME DELAYED DECOUPLED SYSTEM

Specifications	With Decoupler	Without Decoupler
Settling Time (second)	15	50
Rise Time (second)	12	10
% Maximum Overshoot	0	20

TABLE III
TIME RESPONSE ANALYSIS OF SECOND OUTPUT WITH AND WITHOUT DECOUPLER FOR SQUARE TIME DELAYED DECOUPLED SYSTEM

Specifications	With Decoupler	Without Decoupler
Settling Time (second)	50	50
Rise Time (second)	20	20
% Maximum Overshoot	05	25

Robustness Study

Determination of multi - channel output gain margin (MOGM)

MOGM is calculated in this work by varying the multiplicative maximum and minimum gain values to the inputs and outputs of the MIMO plant [25]. In this work 0.65 is minimum value of gain (∂^{min})and 1.42 is maximum value of gain (∂^{max}) for which system is stable. After that, MOGM is calculated as 2.18 and output responses for these gain values are shown in Fig. 7. Fig. 7 (a) and (b) displayed the responses of 1st and 2nd output with the upper gain values respectively whereas the Fig. 7 (c) and (d) portrayed the responses of 1st and 2nd output respectively with lower gain values.

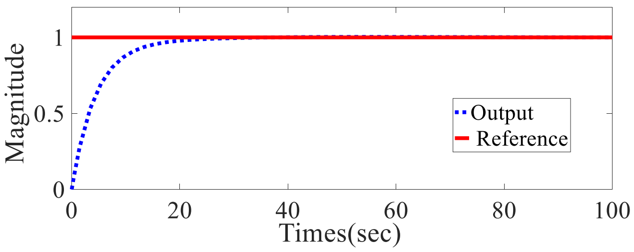

(a) First output plot with maximum gain value

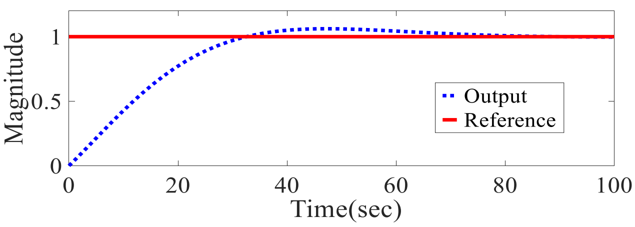

(b) Second output plot with maximum gain value

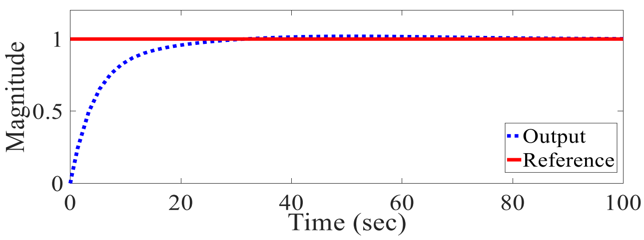

(c) First output plot with minimum gain value

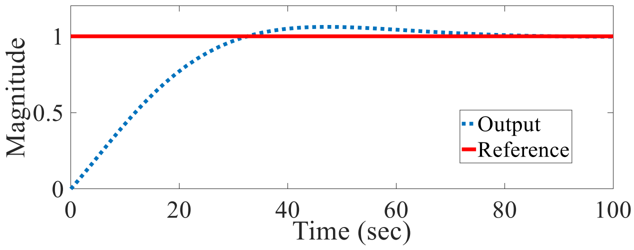

(d) Second output plot with minimum gain value

Fig. 7 Output response for square time delayed decoupled system

Output disturbance rejection

Fig. 8 exhibit the output responses and control signal for the time delayed plant with disturbance rejection. Fig. 8 (a) and (b) displayed the output responses of 1st output and corresponding control signal. Fig. 8 (c) and (d) displayed the output responses of 2nd output and corresponding control signal. It is clearly visible from all the results that due to the output disturbances the performance of the system is not deteriorated.

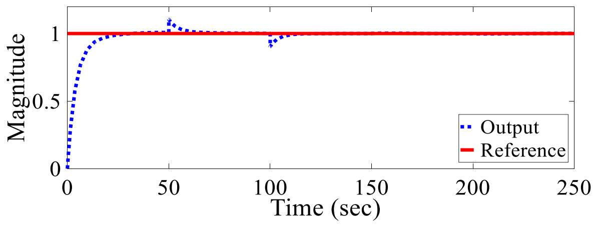

(a) First output plot

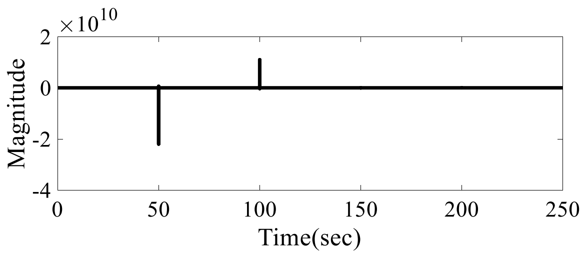

(b) Control signal of first output

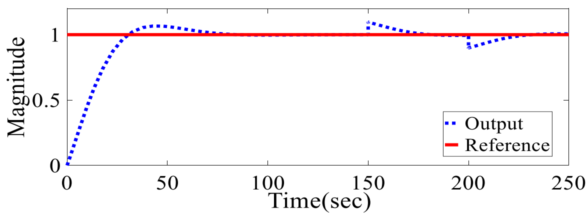

(c) Second output plot

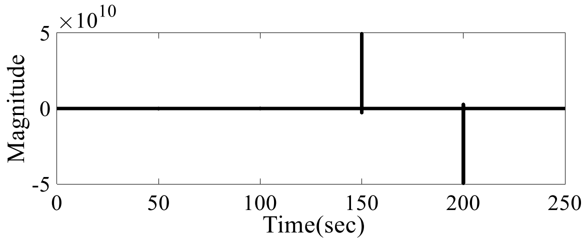

(d) Control signal of second output

Fig. 8. Response of square time delayed decoupled system with output disturbance

B. Non - Square Decoupled System

Considering the transfer matrix obtained in section 2.5.2 after decoupling for controller design. In this controller is designed only for the diagonal plant transfer function $G_{11}(s)$ &$G_{22}(s)$.

$$G_{11}(s) = \frac{4}{20s+1} \tag{46}$$

$$G_{L11}(s) = G_{11}(s).G_{c1}(s)$$
$$= \left[\frac{4K_d s^2 + 20s^2 + 4K_p s + s + 4K_i}{20s^2 + s}\right]$$
$$= s^2[20 + 4K_d] + s[4K_p + 1] + 4K_i \tag{47}$$

The characteristic polynomial of the system is represented by an interval of $[K_{p1}^{-}K_{p1}^{+}]$, $[K_{i1}^{-}K_{i1}^{+}]$, $[K_{d1}^{-}K_{d1}^{+}]$ to determine the range of robustness for K_p,K_i&K_d,respectively, in characteristic polynomial. After it four interval polynomials associated with the Kharitonov characteristic is obtained as below.

$$K_1(s) = s^2[20 + 4K_d^{+}] + s[1 + 4K_p^{-}] + 4K_i^{-}$$

$$K_2(s) = s^2[20 + 4K_d^{+}] + s[1 + 4K_p^{+}] + 4K_i^{-}$$

$$K_3(s) = s^2[20 + 4K_d^{-}] + s[1 + 4K_p^{-}] + 4K_i^{+}$$

$$K_4(s) = s^2[20 + 4K_d^{-}] + s[1 + 4K_p^{+}] + 4K_i^{+} \tag{48}$$

The values of the PID controller gains thus found out are shown in Fig. 9 (a) & 9 (b) for G_{L11} and G_{L22}following the same procedure as discussed in previous example.

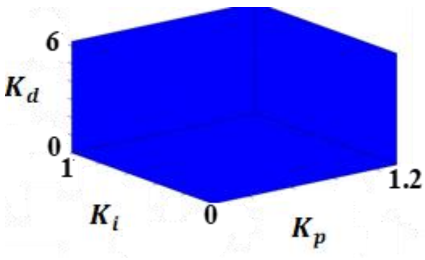

(a) For $G_{L11}(s)$

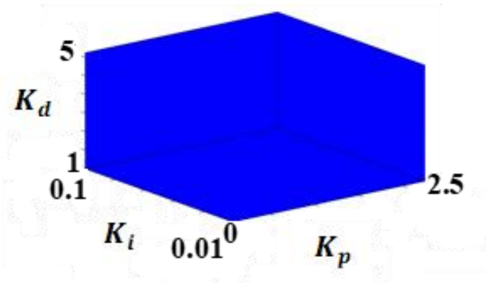

(b) For $G_{L22}(s)$

Fig. 9. PID gain value range for non-square decoupled system

The results are obtained with the optimized value of PID controller using BFO method as discussed previously. Fig. 10 (a) shows the output responses when first input receives a step signal, whereas the second input receives no signal. it is seen that only the 1st output response is obtained whereas the 2nd output response is zero whereas in Fig. 10 (b) output responses is portrayed for such case where second input receives a step signal, whereas the first input receives no signal. It is seen that only the 2nd output response is obtained whereas 1st response is tending to zero. It justified that system is satisfactorily decoupled.

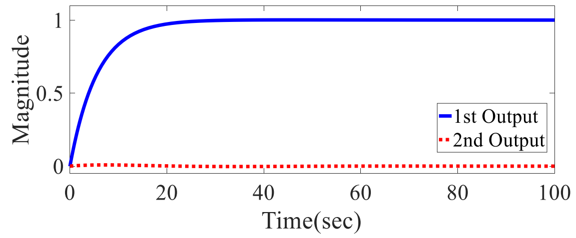

(a) First output's step response and the coupling effect on the second

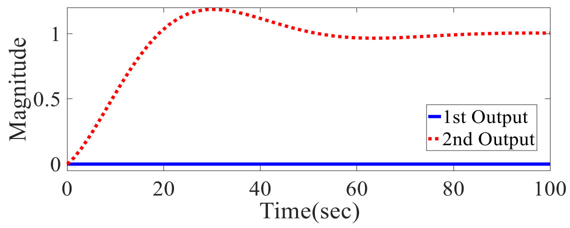

(b) Second output's step response and the coupling effect on the first output

Fig. 10 – Output response of non-square decoupled system

When inputs are applied to both inputs simultaneously, Fig. 11 displays the system's output reaction for both inputs. It is seen from the obtained results displayed in Fig. 11(a) that output response track the reference inputs satisfactorily. Fig. 11 (b) depicts the time response description of both the outputs. Control signals applied for both the outputs are portrayed in Fig. 11 (c). The response of first output with and without the incorporation of decoupler is presented in Fig. 11(d) and the bar charts displayed in Fig. 11 (e) shows the comparative analysis of the output ressponses.

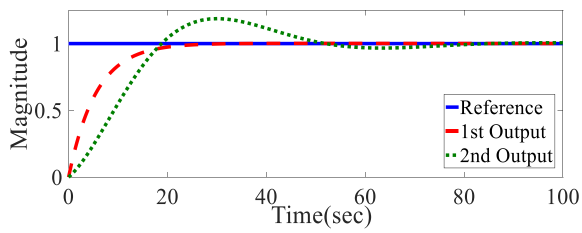

Fig (a) First and Second outputs response

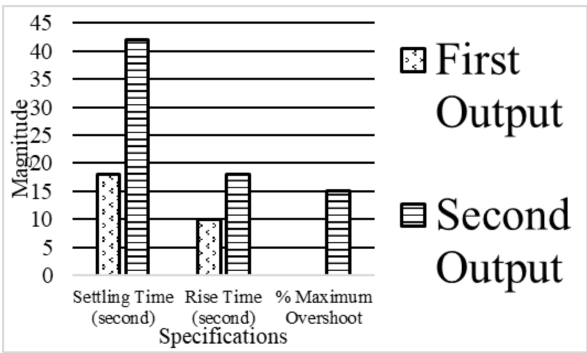

(b) Graphical analysis of the first and second outputs

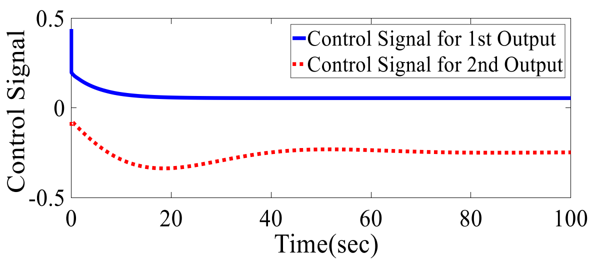

(c) Control signal for first and second outputs

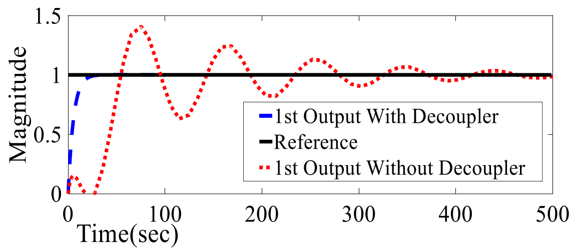

(d) Step response of the first output with and without decoupler

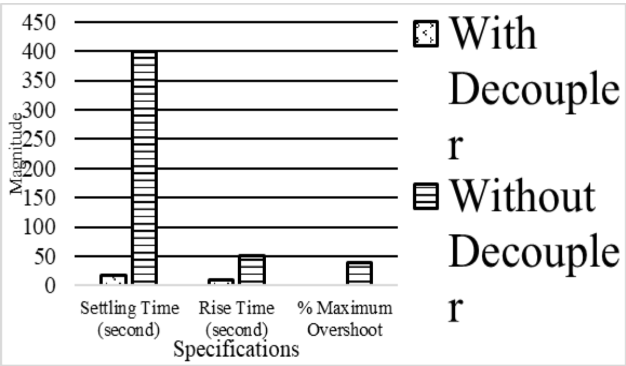

(e) Graphical response analysis of first output with and without decoupler

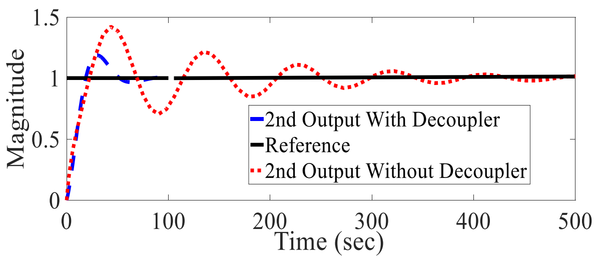

(f) Step response of the first output with and without decoupler

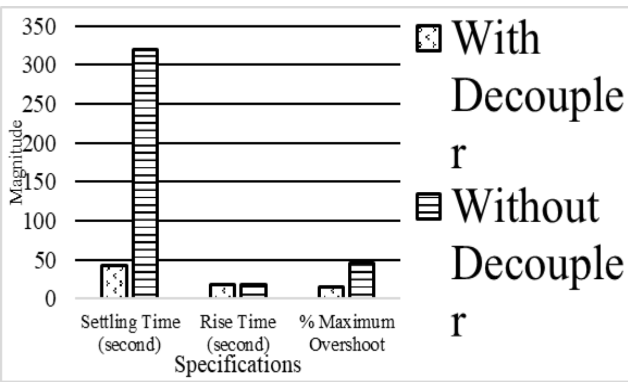

(g) Graphical analysis of second output with and without decoupler

Fig. 11 Time response analysis of non-square decoupled system

Similarly the second output responses with and without decouplers are shown in Fig. 11 (f) and the respective bar chart analysis is portrayed in Fig. 11(g). Time response analysis of the first and second outputs for square time delayed decoupled system is tabulated in Table IV. In Table V time response analysis of first output with and without decoupler for square time delayed decoupled system is tabulated. Table VI depicts the time response analysis of second output with and without decoupler for square time delayed decoupled system.

TABLE IV
TIME RESPONSE ANALYSIS OF THE FIRST AND SECOND OUTPUTS OF NON-SQUARE DECOUPLED SYSTEM

Specifications	First Output	Second Output
Settling Time (second)	18	42
Rise Time (second)	10	18
% Maximum Overshoot	0	15

TABLE V
TIME RESPONSE ANALYSIS OF FIRST OUTPUT WITH AND WITHOUT DECOUPLER OF NON-SQUARE DECOUPLED SYSTEM

Specifications	With Decoupler	Without Decoupler
Settling Time (second)	18	400
Rise Time (second)	10	50
% Maximum Overshoot	0	40

TABLE VI
TIME RESPONSE ANALYSIS OF SECOND OUTPUT WITH AND WITHOUT DECOUPLER OF NON-SQUARE DECOUPLED SYSTEM

Specifications	With Decoupler	Without Decoupler
Settling Time (second)	42	320
Rise Time (second)	18	18
% Maximum Overshoot	15	45

Robustness Study

Determination of MOGM

In this work lower and upper values for gain is determined as (∂^{min}) is 0.55 and (∂^{max}) is 1.65 for the stable system as displayed in Fig.12 which in turns the MOGM to be 3. Fig. 12 (a) & (b) displayed 1st and 2nd output with maximum gain values whereas Fig. 12 (c) & (d) portrayed 1st and 2nd output with minimum values of gains.

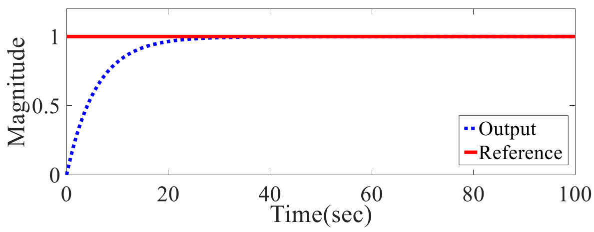

(a) First output's step response using maximum gain value

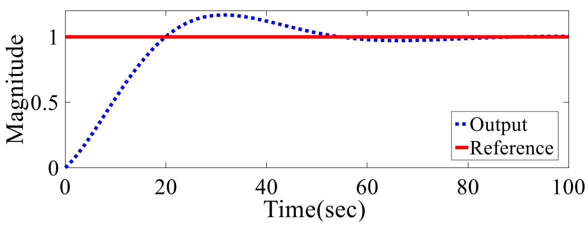

(b) Second output's step response using maximum gain value

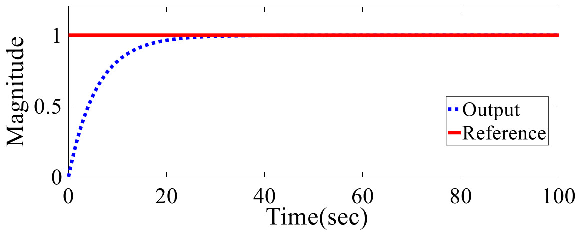

(c) First output's step response using lower gain value

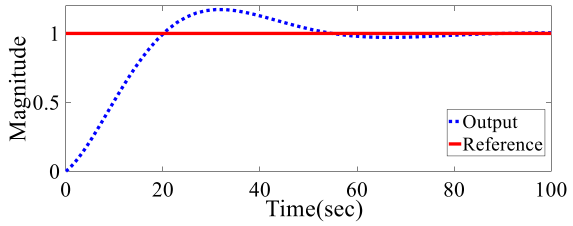

(d) Second output's step response using lower gain value

Fig. 12 Output response of non-square decoupled system

Determination of MODM

The first and second input's delay margin is found as $\tau_{d1} = 0.25$ and $\tau_{d2} = 0.2$. As a result, the multi-channel output delay margin (MODM) is computed to be 0.2. Fig. 13 shows output responses at various levels.

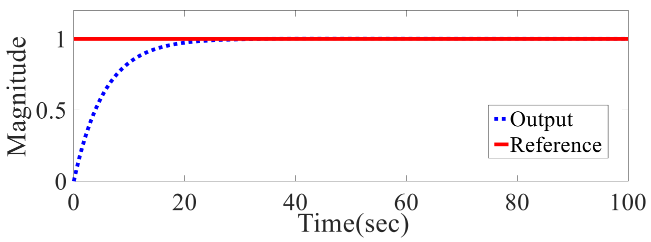

(a) First output response with delay 0.25

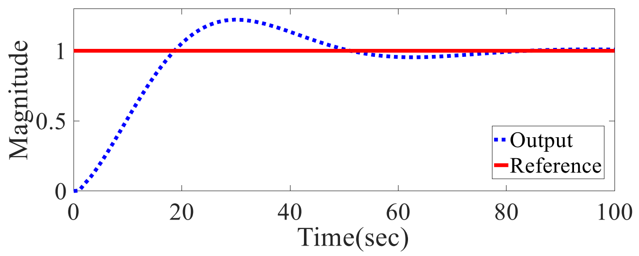

(b) Second output response with delay 0.2

Fig. 13 Output response of non-square decoupled system

Fig. 13 (a) displayed 1st output with a time delay of 0.25 whereas in Fig.13 (b) the output response of 2nd output is displayed with a time delay of 0.2.

Output disturbance rejection

Fig. 14 exhibit the output responses and control signal for the non-square plant with disturbance rejection. Fig. 14 (a) and (b) displayed the output responses of 1st output and corresponding control signal. Fig. 14 (c) and (d) displayed the output responses of 2nd output and corresponding control signal. One can clearly understand from all results that the designed controller is quite capable to exhibit the output disturbance rejection performance.

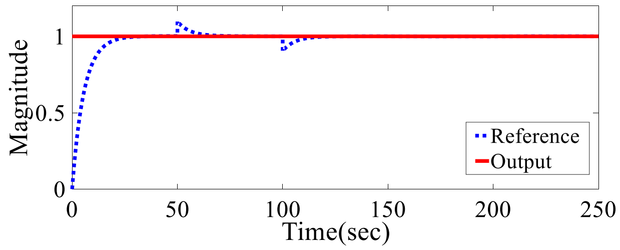

(a) First output plot

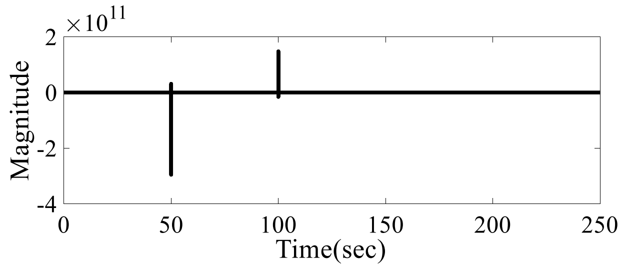

(b) Control Signal of first output plot

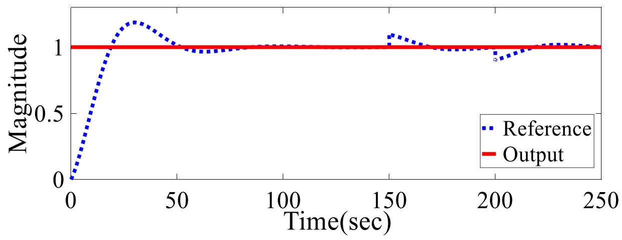

(c) Second output plot

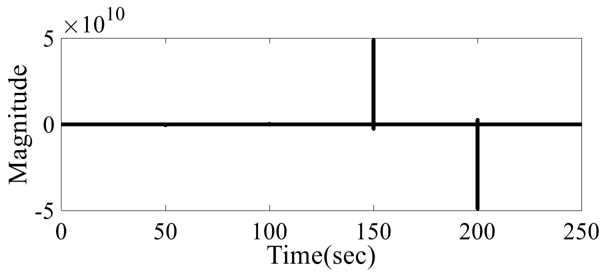

(d) Control signal for second output

Fig. 14 Response of for non-square decoupled system with output disturbance

IV. CONCLUSION

This study provides a comprehensive description of the optimal decoupling and control techniques for various types of MIMO systems. The suggested disentanglement approach is founded upon the principles of LMI and RGA methodology. This approach has demonstrated notable efficacy when evaluating the performance of various types of MIMO systems. The PID controller that has been optimized is also specifically tailored for decoupled MIMO plant, employing Kharitonov theorem and the BFO technique. The method of decoupling control has been effectively executed on several types of plants, including square and non-square plants, plants with time delays, and plants with non-minimum phase characteristics. The robust performance is verified by computation of the MOGM and MODM. The disturbance rejection performance of the designed controller is also tested through output disturbance rejection.

REFERENCES

[1] D. Vaes, J. Swevers, and P. Sas, "Optimal decoupling for MIMO-controller design with robust performance," *Proceedings of the 2004 American Control Conference*, Boston, Massachusetts, 2004.

[2] A. El Garhy and M. El Shimy, "Development of decoupling scheme for high order MIMO process based on PSO technique," *Applied Intelligence*, vol. 26, pp. 217–229, 2007.

[3] N. Abdelkarim, A. Mohamed, A. El-Garhy, and H. Dorrah, "A new hybrid BFOA-PSO optimization technique for decoupling and robust control of two-coupled distillation column process," *Computational Intelligence and Neuroscience*, vol. 2016, pp. 1–17, 2016.

[4] T. Brinsmead and G. Goodwin, "An algebraic approach to optimal output decoupling by output feedback control," *Mathematics Science Institute*, vol. 1, pp. 11–24, 1999.

[5] W. Zhang and C. Lin, "Multivariable Smith predictors design for non-square plants," *IEEE Transactions on Control Systems Technology*, vol. 14, no. 6, pp. 1145–1149, 2006.

[6] A. Ghosh and S. Das Kumar, "Open-loop decoupling of MIMO plants," *IEEE Transactions on Automatic Control*, vol. 54, no. 8, pp. 1977–1981, 2009.

[7] E. Castaneda and J. Ruiz, "Feedback decoupling of linear multivariable systems," *IEEE Latin America Transactions*, vol. 13, no. 8, pp. 2529–2537, 2015.

[8] S. Sato and P. Lopresti, "On the generalization of state feedback decoupling theory," *IEEE Transactions on Automatic Control*, vol. 16, no. 2, pp. 133–139, 1971.

[9] H. Boyd, M. Hast, and K. Astrom, "MIMO PID tuning via iterated LMI restriction," *International Journal of Robust Nonlinear Control*, vol. 26, pp. 1718–1731, 2016.

[10] J. Helton, S. McCullough, M. Putinar, and V. Vinnikov, "Convex matrix inequalities versus linear matrix inequalities," *IEEE Transactions on Automatic Control*, vol. 54, no. 5, pp. 952–964, 2009.

[11] T. Alamo, J. Normey, M. Arahal, D. Limon, and E. Camacho, "Introducing linear matrix inequalities in a control course," *IFAC Proceedings*, vol. 39, no. 6, pp. 205–210, 2006.

[12] G. Leena and G. Ray, "A set of decentralized PID controllers for n-link robot manipulator," *Sadhana*, vol. 37, no. 3, pp. 405–423, 2012.

[13] S. Pandey, J. Dey, and S. Banerjee, "Design of robust proportional-integral-derivative controller for generalized decoupled twin rotor multi-input-multi-output system with actuator non-linearity," *Journal of Systems and Control Engineering*, vol. 232, no. 8, pp. 971–982, 2018.

[14] S. Pandey, J. Dey, and S. Banerjee, "Design and real-time implementation of robust PID controller for twin rotor MIMO system (TRMS) based on Kharitonov's theorem," *1st IEEE International Conference on Power Electronics, Intelligent Control and Energy Systems*, 2016.

[15] S. Bhattacharyya, H. Chapellat, and L. Keel, *Robust Control: The Parametric Approach*. New Jersey: Prentice-Hall, 1995.

[16] L. Fortuna and M. Frasca, *Optimal and Robust Control: Advanced Topics with MATLAB*. CRC Press, 2012.

[17] H. Wang, J. Lam, S. Ding, and M. Zhong, "Iterative linear matrix inequality algorithms for fault detection with unknown inputs," *Proceedings of the Institution of Mechanical Engineers, Part I: Journal of Systems and Control Engineering*, vol. 219, no. 2, pp. 161–172, 2005.

[18] S. Mobayen and D. Baleanu, "Linear matrix inequalities design approach for robust stabilization of uncertain nonlinear systems with perturbation based on optimally tuned global sliding mode control," *Journal of Vibration and Control*, vol. 23, no. 8, pp. 1285–1295, 2017.

[19] H. Abbas, S. Chughtai, and H. Werner, "A hybrid gradient-LMI algorithm for the synthesis of LPV gain-scheduled controllers," *European Control Conference*, vol. 1, pp. 3407–3412, 2009.

[20] A. Ataei and Q. Wang, "An ellipsoid algorithm for linear optimization with uncertain LMI constraints," *American Control Conference*, vol. 1, pp. 857–862, 2012.

[21] H. Hossam, S. Saulat, and W. Herbert, "A hybrid gradient LMI algorithm for solving BMIs in control design problems," *IFAC Proceedings*, vol. 41, no. 2, pp. 14319–14323, 2008.

[22] M. Covacic, M. Teixeira, E. Assuncao, and R. Gaino, "LMI-based algorithm for strictly positive real systems with static output feedback," *Systems & Control Letters*, vol. 61, no. 4, pp. 521–527, 2012.

[23] S. Kumar, I. Kar, and V. Pandey, "Sliding mode controller design for twin rotor MIMO system with a nonlinear state observer," *Proceedings of International Multi-Conference on Automation, Computing, Communication, Control, and Compressed Sensing*, vol. 1, pp. 668–673, 2013.

[24] M. Jahed and M. Farrokhi, "Robust adaptive fuzzy control of twin rotor MIMO system," *Soft Computing*, vol. 17, no. 10, pp. 1847–1860, 2013.

[25] S. Pandey, J. Dey, and S. Banerjee, "Modified Kharitonov theorem-based optimal PID controller design for MIMO systems," *Journal of Electrical Engineering and Technology*, vol. 18, pp. 2317–2334, 2022.

[26] A. Govind and S. Selva Kumar, "A comparative study of controllers for Quanser Qube Servo 2 rotary inverted pendulum system," *Lecture Notes in Electrical Engineering*, vol. 672, pp. 1401–1414, 2020.

[27] S. Adarsh, O. V. Ramana Murthy, and K. R. Sharma, "Analysis of airship dynamics using linear quadratic regulator controller," *15th IEEE India Council International Conference (INDICON)*, India, pp. 1–6, 2018.

[28] S. Adarsh and S. Selvakumar, "Model identification and control of prosthetic leg," *International Conference on Advances in Physical Sciences and Materials*, vol. 1706, no. 1, pp. 2317–2334, 2020.

[29] S. Adarsh and S. Selvakumar, "Model identification and position control of Quanser Qube Servo DC motor," *Advances in Electrical and Computer Technologies*, pp. 1321–1335, 2021.

[30] S. K. Pandey and S. Buyamin, "Edge theorem-based 2-DOF controller design for MIMO system," *Applications of Modelling and Simulation*, vol. 8, pp. 57–69, 2024.

[31] T. S. Chang and A. N. Gaundes, "PID controller synthesis with specified stability requirement for some classes of MIMO systems," *Engineering Letters*, vol. 16, no. 2, pp. 256–265, 2008.

[32] L. Chen, "Parameter tuning of a PID controller based on the cellular genetic algorithm," *Engineering Letters*, vol. 32, no. 4, pp. 828–834, 2024.

[33] G. Chen, X. Tan, Z. Zhang, and Z. Sun, "Parameter optimization of PID sliding mode controller for hydraulic turbine regulating system based on IFABC algorithm," *Engineering Letters*, vol. 28, no. 1, pp. 168–179, 2020.

[34] R. Vilanova, V. M. Alfaro, and O. Arrieta, "Analytical robust tuning approach for two-degree-of-freedom PI/PID controllers," *Engineering Letters*, vol. 19, no. 3, pp. 204–214, 2011.